Physical properties of the GexSe1 − x glasses in the 0 < x < 0.42 range in correlation with their structure

Guang Yang, Yann Gueguen, Jean-Christophe Sangleboeuf, Tanguy Rouxel, Catherine Boussard-Plédel, Johann Troles, Pierre Lucas, Bruno Bureau

Physical properties of the Ge_xSe_{1-x} glasses in the 0<x<0.42 range in correlation with their structure

Guang Yang[1,2], Yann Gueguen[1,*], Jean-Christophe Sangleboeuf[1], Tanguy Rouxel[1], Catherine Boussard-Plédel[2], Johann Troles[2], Pierre Lucas[3], Bruno Bureau[2]

1. LARMAUR ERL CNRS 6274, Universités de Rennes 1, Campus de Beaulieu, 35042 Rennes Cedex, France

2. UMR CNRS 6226 Sciences Chimiques de Rennes, Groupe Verres et Céramiques, Université de Rennes I, Campus de Beaulieu, 35042 Rennes Cedex, France

3. Department of Materials Science and Engineering, University of Arizona, 4715 E. Fort Lowell Road, Tucson, Arizona 85712, USA

**Corresponding author:* Tel.: +33 2 23 23 58 06; fax: +33 2 23 23 61 11. E-mail address: yann.gueguen@univ-rennes1.fr (Y. Gueguen).

Abstract

Physical properties, including mechanical, thermal and optical properties, have been investigated for chalcogenide glasses in the Ge_xSe_{1-x} system, for x ranging between 0 and 0.42. In the $0<x<1/3$ range, the elastic moduli or the glass transition temperature (T_g) evolve as would be expected from the chain crossing model or from the clustering model. The change is continuous and there is no incidence of the rigidity percolation threshold (<r>=2.4). Conversely, the chemical threshold (<r>=2.67) clearly induces a change in the compositional trend of these properties. In the $x>1/3$ range, T_g decreases and the elastic moduli markedly increase, which is not expected from the continuously reticulated model. The change of the physical

properties in this range is an indicator of the existence of separated Ge-rich domains.

Keywords: chalcogenide glasses; elastic moduli; structure; glass transition

1. Introduction.

Chalcogenide glasses have attracted a wide interest of the researchers for several decades due to a variety of technological applications in infrared optics. The large forming region permits to tune physical properties (such as, optics, electronic and mechanical) over a wide range of composition. Physical properties are controlled by the glassy structure, therefore a detailed knowledge of the short and intermediate range structure is important to make useful models of structure-property correlation.

Although a lot of insightful research has been conducted on these glass [1][2][3][4][5][6][7][8][9], the structure of binary Ge_xSe_{1-x} glasses remains quite controversial. Previous reports have suggested two major extreme models were proposed to describe their structure, especially in Se-rich region (x<1/3): the chain crossing model (CCM) and the clustered model (CM). The CCM is based upon $GeSe_{4/2}$ tetrahedral units uniformly distributed in the glassy network and linked through corners by short Se chains. In contrast, the CM is based on the aggregation of corner or edge shared $GeSe_{4/2}$ tetrahedra (CS and ES respectively) on one hand and the presence of longer Se_n chains and rings on the other hand. The CCM fails to explain the existence of CS and ES $GeSe_{4/2}$ units in Se-rich compositions as observed by Raman spectroscopy and the ^{77}Se NMR results also disagree with the “ideal” CCM

and privilege the existence of glassy domains richer in tetrahedra releasing the excess of Se [8],[10].

Generally speaking, the structure of selenide glasses is commonly described as a network of covalent bonds obeying the 8-N rule. Based on this assumption, the rigidity percolation theory predicts that a structural threshold is reached for an average coordination value of <r> = 2.4 ($<r> = \Sigma_i x_i r_i$; x_i being the atomic fraction of atoms i and r_i the coordination number of these atoms). However, the constrained counting scheme [11] leads to a percolation threshold at <r> = 2.4 only in the frame of the ideal CCM. This is the reason why, in order to justify the absence of sharp transition at <r> = 2.4, models departing from an ideal CCM have been developed [12]. Nevertheless, spectroscopic techniques (Raman and NMR), and also molecular dynamic calculation, do not confirm at all the validity of the CCM in Ge_xSe_{1-x} glasses. In that context, it appeared interesting to track down any special physical features occurring around <r> = 2.4 (corresponding to $Ge_{0.2}Se_{0.8}$), to test the effect of rigidity at this glass stoichiometry. In particular, structural rigidity would be expected to directly affect mechanical properties such as elastic properties. It is also interesting to compare the relative effect of the stoichiometry on these properties. Both the CCM and the CM are limited to the domain where $x<1/3$ in Ge_xSe_{1-x} glasses, since at $x=1/3$ a network of interconnected $GeSe_{4/2}$ tetrahedra is expected (both models lead to this conclusion). $x=1/3$ corresponds to the chemical threshold (<r> = 2.67), at which germanium cannot be added without forming homopolar bonds. So, it seemed to be also interesting to study the impact of this chemical threshold on the physical properties.

In the past, several authors proposed thermo-mechanical measurements and interesting analysis on the Ge-Se glasses, but as part as broader studies including numerous glass compositions [13],[14],[15],[16] and most of the time, very few binary glass compositions rich in Ge (beyond $GeSe_2$) had been prepared and considered.

In this paper, a whole set of physical properties including elastic moduli, glass transition temperatures, densities, refractive indexes and band-gap energies were measured for a complete series of Ge_xSe_{1-x} glasses, from Se to $Ge_{0.42}Se_{0.58}$, all prepared following the same procedure. Thus, in this contribution, the authors propose to revisit these physical measurements, focused on a controversial simple binary system, by rationalizing and enriching them. Various models are contrasted with the experimental data. This exhaustive work on the Ge_xSe_{1-x} glasses complements and supplements a previous equivalent work recently published on the As_xSe_{1-x} glasses [38].

2. Experiments

Ge_xSe_{1-x} glassy rods (20 to 25 *g*) of composition x= 0, 0.10, 0.20, 0.25, 1/3, 0.36, 0.38, 0.40 and 0.42 were prepared in evacuated fused silica ampoules by conventional melt-quenching method [4]. The glassy nature of the obtained glasses was confirmed by X-ray diffraction analysis and the optical homogeneity was verified with a thermal-imaging camera. The compositions of as-made glasses were analyzed by Energy Dispersive X-Ray Spectroscopy (EDS) using a JEOL JSM 6400 electron microscope and analysis software from EDS OXFORD INCA Corporation.

Differential scanning calorimetry (DSC) measurement (TA DSC Q20, TA Instruments, Castle, USA) was conducted at a heating rate of 10 K /min under an Ar atmosphere at ambient pressure.

The glass densities ρ at 20°C were measured by the Archimedes method using de-ionized water as the immersion fluid. The atomic volume is calculated using the density and the molar weight ($V=(\Sigma_i x_i M_i)/\rho$; x_i being the atomic fraction of atoms i and M_i the molecular weight of these atoms). The elastic moduli were calculated from the measurements of the longitudinal, V_l, and transverse, V_t, ultrasonic wave velocities, at 20°C, with a relative error better than ± 2% using 10 MHz piezoelectric transducers. Young's modulus E, shear modulus G, bulk modulus K, and Poisson's ratio ν, were derived from the classical elasticity relationships [17]:

$$E = \rho\,(3\,V_l^2 - 4\,V_t^2)/((\,V_l/\,V_t)^2 - 1) \qquad (1.1)$$

$$G = \rho\,V_t^2 \qquad (1.2)$$

$$\nu = E/(2G) - 1 \qquad (1.3)$$

$$K = E/(3(1-2\,\nu)) = E/(9-3E/G) \qquad (1.4)$$

We have also investigated the composition dependence of the glassy refractive index, n, and of the glassy optical band gap, E_g, for Ge_xSe_{1-x} glasses, using the transmission spectra. The indexes of refraction were measured at 1.3 and 1.54 µm with a Metricon prism coupler. The optical band gaps were evaluated directly from the transmission curve using Tauc plot.

3. Results

3.1 Glass transition temperatures and crystallization

From the DSC curves in Figure 1, the glass transition temperature (T_g) and the point of maximum crystallization (T_x) were obtained. The glass transition temperature continuously increases, as the Ge content increases in the Ge_xSe_{1-x} system, with a maximum at x = 1/3, and then continuously decreases. These measurements are in very good agreement with those of Boolchand *et al.* [18], with some extension in the Ge-rich domain. Ge-rich Ge_xSe_{1-x} glasses show large crystallization peaks, with a shoulder for x = 0.40 and even two crystallization peaks for x = 0.42. By comparing the XRD spectra of the $Ge_{0.42}Se_{0.58}$ glasses annealed at 400 °C and at 460 °C for 10 h, and the XRD spectra of GeSe and $GeSe_2$ crystals, we can attribute the first crystallization peak (lowest temperature) to the crystallization of GeSe, and the second one to the crystallization of $GeSe_2$.

3.2 Elastic moduli

Similarly, Young's modulus E and shear modulus G exhibit a continuous increase in the ranges of $0<x<1/3$ but, as opposed to T_g, still increase in the $1/3<x<0.42$ range, but with a different slope, while Poisson's ratio ν keeps decreasing through the whole composition, as shown in Figure 2. This is consistent with the measurements of Yun *et al.* [19] in the $0<x<1/3$ range, and the measurement of the shear elastic moduli

proposed by Duquesne *et al.* [20] in the $0<x<2/5$ range.

3.3 Density

Compared with T_g and elastic moduli, the density or the atomic volume exhibits a non-monotonic evolution with x as shown in Figure 3. The density increases in the range of $0<x<0.2$, then decreases in the range $0.2<x<0.33$, and finally increases in the range of $0.33<x<0.42$, therefore showing two extrema, a minimum at $<r>=2.4$ and a maximum at $<r>=2.67$. This confirms the trend observed by various authors [17],[21],[22].

3.4 Optical properties

Figure 4 reveals that the short wavelength absorption edge takes a maximum value at around $x= 1/3$, which is in agreement with the previous reports [23],[24],[25] for the band-gap energy (E_g) of Ge_xSe_{1-x} glasses. E_g is connected to the network connectivity, its density and to the mean bonding energy [25]. The band-gap energy is supposed to increase with the bonding energy (U) [26],[27], and thus increases in the $x<1/3$ range, since $U_{Ge-Se}>U_{Se-Se}$. But this is probably not the major factor, since the maximum does not correspond to the glass possessing the highest mean bonding energy. In fact, the valence band of Se-rich Ge_xSe_{1-x} glasses is formed by selenium lone-pair orbital, which are non-bonding in nature and have higher energy than the bonding ones. As for the conduction band, it is constituted of the antibonding states. In one words, the E_g is related to lone-pair electrons rather than to the bonding energy

level. In the germanium-rich range (x>1/3), E_g decreases because the degree of crosslinking increases [25], thus increasing the intermolecular interaction, widening the separation between the bonding and anti-bonding states. Figure 4 also depicts compositional dependences of the n indexes showing a minimum at x=1/3, which roughly corresponds to the change of bulk glassy atomic volume, although it notably lacks a maximum at <r>=2.4. In fact, it seems that the refractive index follows the reverse trend of the band-gap. This is not unexpected, regarding the Wemple and DiDomenico single oscillator model, using simple assumptions in order to correlate the parameters of this model with the band-gap energy [28].

4. Discussion

4.1 CCM vs. CM

None of the physical properties measured here tend to favor of the Chain Crossing (CCM) versus the Clustering Model (CM). Indeed, these physical properties reflect the macroscopic behavior of glasses, and can be connected to the mean atomic bonding energy, or its density. As the Ge content increases, four-fold Ge atoms substitute for two-fold Se atoms and since the $U_{Ge\text{-}Se}$= 215 kJ/mol and $U_{Se\text{-}Se}$= 184 kJ/mol [29], an increase of the bonding energy follows. Consequently, in the 0<x<1/3 range, the glass network becomes more and more cross linked, with higher and higher mean bonding energies, whatever the model considered. When x>1/3, homopolar Ge-Ge bonds form, with lower bonding energy ($U_{Ge\text{-}Ge}$= 157 kJ/mol [29]). Thus, the changes of all the physical properties, in the 0<x<1/3 range are consistent with mean

bonding energy and mean coordination number increases: T_g increases, due to an increase of the mean bonding energy and in the present case, this corresponds to a network connectivity increases [30]; the elastic moduli increase with the volume density of bonding energy [31]; Poisson's ratio decreases as the network connectivity increases [32]; and the refractive index of a glass is supposed to increase with enhancing its mean bonding energy and/or density because of higher electronic density.

Nevertheless, the density follows a trend that neither the CCM nor the CM can explain. The local maximum of density at x=0.2 (the percolation threshold) could results from the existence of specific dense structures, such as two edge shared-$GeSe_{4/2}$ tetrahedra interconnected with four corner shared-$GeSe_{4/2}$ (outrigger raft structure)[6],[33], where extra Se atoms occupy the free volumes [6]. But it is rather difficult to justify a maximum concentration of these structures at x=0.2, when the ratio of ES/CS continuously increases with x in the $0<x<1/3$ range [34]. Moreover, the local maximum of density at, or close to the percolation threshold seems to be universal among chalcogenide glasses [15],[25]. Thus, the universality of this maximum can only be associated with the optimized network constraint around the percolation threshold. The evolution of the band-gap energy is also rather difficult to explain, since we expect to observe a decrease when the network connectivity increases [25]. Indeed, in Ge-S, As-Se, and As-S glasses, E_g decreases when x increases in the $0<x<1/3$ range [25]. The As-Se glasses are nicely described by the CCM [35] and the As-S glasses are close to be described by the CCM [36]. Since the

Ge_xSe_{1-x} glasses follow the opposite trend, we may suppose a large departure from the CCM for this system. Nevertheless, the CCM fails also to describe the structure Ge-S glasses (see [37],[38] for an example), for which a phase separation of S_8 rings is proposed. According to Tanaka [25], the unexpected trend of the Ge-Se glasses could also result from the relatively small density evolution in the $0<x<1/3$ range.

Hence, in the $0<x<1/3$ range, the physical properties do not clearly favor one structural model over the other. Nevertheless, recent ^{77}Se NMR and Raman studies [8],[39] rather suggest that the structure of Ge_xSe_{1-x} glasses is close to a statistically random connectivity model (SRCM) in the $0<x<1/3$ range: -Se-Se- linkage exists between $GeSe_{4/2}$ edge and corner shared tetrahedra [8],[9],[10]. However, the measurement of the fraction of the different Se sites also point out a small deviation from the SRCM, indicating that the glass structure is somewhere between the SRCM and the CM [39] (i.e.: that few Se-chains do not presumably connect the $GeSe_{4/2}$ tetrahedra).

4.2 Percolation threshold

The idea of the existence of a rigidity percolation threshold in the physical properties of chalcogenide glasses has emerged from the model of Philipps and Thorpe [11],[40]. By counting the angular and the stretching constrains per atom, we can estimate the average coordination number where the number of constrains per atom is equal to the number of degrees of freedom: $<r>=2.4$ ($x=0.2$ in the Ge_xSe_{1-x} system). This topological approach being based on the calculation of mechanical

constrains, He and Thorpe [41] have suggested that the percolation threshold (being also called “rigidity” or “mechanical” percolation threshold) should correspond to a second order transition (change in slope) in the evolution of the elastic moduli of glasses. While this has been initially verified in the Ge-As-Se [42] subsequent studies have revealed different trends [13],[43] and elastic moduli measured experimentally in binary systems [19] have not showed any trend at <r>=2.4. More generally speaking, it seems that the elastic constant are only sensitive to the chemical threshold [14]. The elastic moduli measured here clearly agree with this conclusion: neither the Young modulus, nor the shear elastic modulus, nor the Poisson ratio, and thus the bulk elastic modulus, indicates a second order transition at <r>=2.4 in the Ge_xSe_{1-x} system. So, the physical property that should be most evidently connected to the constraint theory does not give any signature of the threshold predicted by this model. The evolution of the elastic moduli measured here clearly confirms that there are not at all controlled by the floppy modes in Ge_xSe_{1-x} glasses [44]. Even the hardness [17], does not provide an evidence of a mechanical effect of the percolation threshold in this system.

The T_g is not supposed to be directly sensitive to the average constrains, but only to the network connectivity [30] and so does not provide any signature of the percolation threshold either. The refractive index is also insensitive to this topological aspect and does not highlight the percolation threshold.

Nevertheless, the band-gap energy shows a transition at <r>=2.4, but as suggested by Tanaka [25], this could be connected to the intermolecular distance impacting the valence energy, and so to the density or atomic volume. Indeed, the density itself shows an extremum at <r>=2.4, this is observed in many chalcogenide systems [45]. The density appears to be the only physical property that shows a systematic signature of the rigidity percolation threshold in various binary and ternary chalcogenide systems. However, based on the premises of the theory, it is rather difficult to identify a direct connection between the structural rigidity and the packing density. Overall, the most significant extrema, regarding the band-gap energies or the densities corresponds to <r>=2.67 (x=1/3). Actually, all the physical properties show a drastic change in their slope, at least, at <r>=2.67.

4.3 Glass transition temperature and elastic moduli

The glass transition temperature and the elastic moduli both undergo an important change at <r>=2.67, but with a very different behavior. The T_g, E and G all increases with x (or <r>) in the $0<x<1/3$ domain, but at $x>1/3$, the T_g decreases while E and G drastically increase. The T_g is mainly controlled by the connectivity and the mean bonding energy, while the elastic moduli are controlled by its volume density (i.e.: the mean bonding energy per unit volume). At x=1/3, the glass network is supposed to be only formed by $GeSe_{4/2}$ tetrahedra. So, it could be argued that increasing the Ge content will lead to the formation of Ge-Ge homopolar bonds [39] with a lower bonding energy than Ge-Se bonds, and thus, inducing a T_g decrease. As depicted on Figure 3, the atomic volume also drastically decreases in the $x>1/3$ domain, so we

could also argued that it compensates the mean bonding energy decrease, and increases the elastic moduli.

However, the mean bonding energy itself is not sufficient to understand the evolution of T_g. As underlined by Boolchand et al. [30], the difference in bonding energies between Ge-Ge bonds and Se-Se bonds is very close to the difference between Si-Si and Si-Se bonds. Despite this similarity, the T_g of Si_xSe_{1-x} glasses does not decrease at x=1/3. It underlines that structural specificities come into play, impacting on T_g, such as nanoscale phase separation [30]. Models including the temperature dependence of topological constraints have also successfully reproduced this trend [46].

4.4 Mean atomic bonding energies

Since the glass transition temperature itself is probably not sufficient to arbitrate between a nanophase separated or a continuously reticulated model (CRM), we will take a deeper look at the mean bonding energies. The atomic bonding energy per mol atoms is directly related to the bulk modulus and the atomic volume at equilibrium. In the simplistic case of a Mie-Grüneisen potential, the first Grüneisen rule [47] gives:

$$K = m\, nU_0/(9V_0) \qquad (1.1)$$

where U_0 is the atomic bonding energy, V_0 is the atomic volume at equilibrium, and m and n are the exponents of the power law describing the attractive and the repulsive terms, respectively. It is interesting to compare the theoretical prediction with the experimental results assuming for instance that $m\, n /9 \approx 1$ (n=1, for the Coulomb

attraction, and m=9, see ref.[48]), in order to compare theoretical and actual trend. Obviously, because this is a very simplistic approach, we do not expect to exactly reproduce the evolution of the bulk modulus, but this calculation will provide a trend that can give indications regarding the glass structures. We can first estimate an experimental mean bonding energy (U_{0exp}), from the bulk elastic modulus and the atomic volume. Then, using the Se-Se, Ge-Ge and Ge-Se bonding energies, the possible structural units in the Ge_xSe_{1-x} system according to the CCM (for the $0<x<1/3$ range) and the CRM (for $x>1/3$), we can estimate the theoretical mean bonding energies and compare them to the experimental one. In the CRM, the two-fold Se atoms are continuously substituted by four-fold Ge atoms in $GeSe_{4/2}$ tetrahedra, so that the possible structural units are clearly identified. We have used experimental values of inter-atomic bonding energy obtained by calorimetry in ref. [49] (U_{01}) and [29] (U_{02}) to estimate the mean energy bonding from CCM and CRM. The method used to calculate the mean bonding energies is detailed in ref. [50].

The mean atomic bonding energies are plotted on Figure 5. As expected, both the experimental and theoretical show a transition at $x=1/3$. Moreover, in the $0<x<1/3$ range, the continuous increases of the experimental U_{0exp} is consistent with the continuous T_g increase, and the continuous increase of U_{01} and U_{02} is consistent with the continuous increase of the elastic moduli. Nevertheless, U_{0exp} drastically increases in the $x>1/3$ range, this indicates that the low bonding energy of Ge-Ge bond is largely compensated by the increase in network connectivity. U_{01} and U_{02} increase in the $x>1/3$ range, but very slowly. This is in contradiction with the T_g decrease, this

confirming a possible phase separation. Note that in the Si_xSe_{1-x} system, the T_g continuously increases as x increases, but more slowly in the x>1/3 range [30], exactly like the theoretical U_0 of the Si_xSe_{1-x} glasses (the trend of the theoretical U_0 of Si_xSe_{1-x} glasses looks like the one of the Ge_xSe_{1-x} glasses, since the difference in bonding energy between Ge-Ge bonds and Se-Se bonds and between Si-Si and Si-Se bonds is very close [30]). This indicates that the CRM fails to describe the structure of Ge-rich Ge_xSe_{1-x} glasses.

In order to dig deeper in this analysis, we have calculated the mean atomic bonding energy densities ($U_1=U_0/V_0$) to compare the theoretical U_1 expected from the CRM with the one deduced from the experimental elastic moduli (U_{1exp}). The mean atomic bonding energies are reported on Figure 6. The large decrease of molar volume in the x>1/3 range (Figure 3) compensates the slow increase of U_{01} and U_{02} in this domain, but not in a sufficient way to explain the drastic increase of the elastic moduli in this range. Again, it seems that the CRM fails for Ge-rich Ge_xSe_{1-x} glasses.

4.5 Structural suggestion for Ge-rich glasses

The structure of the $GeSe_2$ glass has been studied for a long time (see ref. [51] and references therein). There are strong evidences that the structure of the $GeSe_2$ glass itself does not correspond to the ideal network of $GeSe_{4/2}$ tetrahedra, since Ge-Ge homopolar bonds are already present, in a non-negligible fraction (>2%) [51], and since Se-Se bonds still exist [39]. ^{119}Sn Mössbauer spectroscopy, Raman spectroscopy and the evolution of the T_g all suggest the existence of $Ge_2(Se_{1/2})_6$ nanophases in the

320 x>1/3 range [51]. Consequently, we could not expect that the evolution of the physical properties of Ge-rich Ge_xSe_{1-x} glasses will correspond to a substitution of Se atoms by Ge atoms in a $GeSe_{4/2}$ tetrahedra network. Thus, this evolution will not have a trend similar to the transition from the $GeSe_2$ β-crystal to the Ge crystal. On Figure 7 we have reported the evolution of the density of Ge-rich Ge_xSe_{1-x} glasses, with those of
325 $GeSe_2$, GeSe, and Ge crystals. It clearly appears that the slope of the density *vs.* x is closer to the evolution from the $GeSe_2$ crystal to the GeSe crystal, than to the Ge crystal. In other words, this slope does not correspond to substitution of Se atoms by Ge atoms in a $GeSe_{4/2}$ tetrahedra network, so does not correspond to the CRM. This is consistent with the recent ^{77}Se NMR study [39] showing that the Ge-Ge bonds are not
330 homogenously distributed in the network. We have also reported the evolution of the mean atomic bonding energy density of Se, $GeSe_2$, GeSe, and Ge crystals. From the CCM and the CRM, we expect the bonding energy density of glasses to follow an almost continuous line from x=0 to x>1/3, exactly like the line ($dU_1/dx \approx 0{,}14$ kJ/cm^3/x) joining the Se, $GeSe_2$ and Ge crystals on Figure 7. The experimental
335 bonding energy density drastically increases at x=1/3 ($dU_1/dx \approx 0{,}48$ kJ/cm^3/x), and does not follow the line expected from the CRM. The slope of this increase, in the x>1/3 range, is closer to the change of bonding energy density between the $GeSe_2$ and the GeSe crystal ($dU_1/dx \approx 0{,}43$ kJ/cm^3/x). These trends, regarding the densities and the mean atomic bonding energies, suggest the existence of clusters similar to GeSe
340 crystal (a distorted rock salt structure with three fold Ge and Se atoms), or at least the existence of phase separated domains explaining the departure from the trend

expected from the CRM. The first crystallization peak of the $Ge_{0.42}Se_{0.58}$ glass, corresponding to the GeSe crystal, could also support this; although the crystallization of a certain phase doesn't necessary imply that the glass structure is similar to this phase.

5. Conclusion

We have investigated the physical properties of Ge_xSe_{1-x} glasses in the range of $0 \leq x \leq 0.42$. We do not observed any impact of the rigidity percolation threshold (<r>=2.4), predicted by the model of constrain counting of Philipps and Thorpe [11][40], on the elastic moduli, on T_g, or on the refractive index. On the other hand, the density shows a local minor extremum around <r>=2.4 (or x=0.2), probably explaining why the band-gap energies suddenly increases at x=0.2. Nevertheless, the relationship between the rigidity threshold and the density is not as obvious as it should be with the elastic moduli. The evolution of the elastic moduli and of the T_g, in the $0<x>1/3$ is consistent with the continuous increase of the network connectivity, of the mean atomic bonding energy and of its density, according to both the chain crossing model (CCM) and the clustered model (CM). The chemical threshold, at <r>=2.67 (or x=1/3), impacts all the physical properties measured here, corresponding to a extremum of all of them, except for the elastic moduli showing, instead, a marked change in their slopes. In the x>1/3 range, the T_g and the elastic moduli do not follow the expected trends according to a continuously reticulated model (CRM) where the

Se atoms of $GeSe_{4/2}$ tetrahedra are substituted by Ge atoms. Their trend, instead, supports the existence of Ge-rich domains, separated from the glassy network, as suggested by Boolchand *et al.* [51]. These phase-separated domains induce a loss of network connectivity, thus decreasing the T_g but also contribute to a dense structure with a large density of mean atomic bonding energy, thus increasing the elastic moduli markedly, as compare as what is expected from a CRM.

Acknowledgements

This work has been supported by the National Science Foundation (NSF Grant# ECCS- 1201865).

References

[1] P. Tronc, M. Bensoussan, A. Brenac, C. Sebenne, *Phys. Rev. B, 8* [12], (1973), 5947-5956

[2] P. Boolchand, W. J. Bresser, *Philos. Mag. B, 80*[10], (2000), 1757-1772,

[3] B. Bureau, J. Troles, M. Le Floch, P. Guenot, F. Smektala and J. Lucas, *J. Non-Cryst. Solids, 319*[1-2], (2003), 145-153

[4] B. Bureau, J. Troles, M. Le Floch, F. Smektala and J. Lucas, *J. Non-Cryst. Solids, 326-327,* (2003), 58-63

[5] P. Boolchand, P. Chen, M. Jin, B. Goodman and W.J. Bresser, *Phys. B: Cond. Matter, 389*[1], (2007), 18-28

[6] R. Golovchak, O. Shpotyuk, S. Kozyukhin, A. Kovalskiy, A.C. Miller and H. Jain, *J. Appl. Phys.*, *105*[10], (2009), 103704

[7] P. Lucas, E. A. King, O. Gulbiten, J. L. Yarger, E. Soignard and B. Bureau, *Phys. Rev. B*, *80*[21], (2009), 214114

[8] E.L. Gjersing, S. Sen and B. G. Aitken, *J. Phys. Chem. C*, *114*[18], (2010), 8601-8608

[9] M. Kibalchenko, J. R. Yates, C. Massobrio and A. Pasquarello, *Phys. Rev. B*, *82*[2], (2010), 020202

[10] M. Kibalchenko, J. R. Yates, C. Massobrio and A. Pasquarello, *J. Phys. Chem. C 115*, (2011), 7755

[11] M.F. Thorpe, *J. Non-Cryst. Solids*, 57, (1983), 355-370

[12] C. Massobrio, M. Celino, P. S. Salmon, R. A. Martin, M. Micoulaut and A. Pasquarello, *Phys. Rev. B*, 79, (2009), 174201

[13] A.K. Varshneya, A.N. Seeram and D.R. Swiler, *Phys. Chem. Glasses*, 34 [5], (1993), 179-192

[14] S. Mahadevan and A. Giridhar, *J. Non-Cryst. Solids*, 110, (1989), 118-121

[15] S. Mahadevan and A. Giridhar, *J. Non-Cryst. Solids*, 143, (1992), 52-58

[16] U. Senapatia and A.K. Varshneya, *J. Non-Cryst. Solids*, 185, (1995), 289-296

[17] J. P. Guin, T. Rouxel, V. Keryvin, J.-C. Sangleboeuf, I. Serre and J. Lucas, *J.*

Non-Cryst. Solids, *298*, (2002), 260-269

[18] P. Boolchand, X. Feng and W. J. Bresser, *J. Non-Cryst. Solids*, *293-295*, (2001), 348–356

[19] S.S. Yun, H. Li, R.L. Cappelletti, R.N. Enzweiler and P. Boolchand, P. *Phys. Rev. B*, *39*, (1989), 8702-8706

[20] J.Y. Duquesne and G. Bellessa, *Europhys. Lett.*, 9 [5], (1989), 453-458

[21] Y. Ito, S. Kashida and K. Murase, *Solid State Comm.*, *65* [6], (1988), 449-452

[22] R. Azoulay, H. Thibierge and A. Brenac, *J. Non-Cryst. Solids*, *18*, (1975), 33-53

[23] W.Zhou, M. Paesler and D. E. Sayers, *Phys. Rev. B*, *43* [3], (1991), 2315

[24] I. Petri, P.S; Salmon and H.E. Fischer, *Phys. Rev. Letter*, *84* [11], (2000), 2413

[25] K. Tanaka, *Phys. Rev. B*, *39*, (1989), 1270-1279

[26] M. Kastner, *Phys. Rev. Lett*, 28, (1972), 355-357

[27] G. Saffarini, J.M. Saiter, H. Schmitt, *Opt. Mater.*, 29,(2007), 1143-1147

[28] H. Tichá, L. Tichy, *J. Optoelectron. Adv. M.,* 4 [2], (2002), 381-386

[29] L. Pauling, "The Nature of the Chemical Bond." Ithaca, NY: Cornell University Press. (1960)

[30] P. Boolchand, D.G. Georgiev, T. Qu, F. Wang, L. Cai and S. Chakravarty, *C. R. Chimie*, *5*, (2002), 713 – 724

[31] T. Rouxel, *J. Am. Ceram. Soc.*, *90*, (2007), 3019-3039

[32] T. Rouxel, H. Ji, T. Hammouda and A. Moreac, *Phys. Rev. Lett.*, 100, (2008), 225501

[33] P. M. Bridenbaugh, G. P. Espinosa, J. E. Griffiths, J. C. Phillips and J. P. Remeika, *Phys. Rev. B*, 20[10], (1979), 4140

[34] T. G. Edwards and S. Sen, *J. Phys. Chem. B*, 115, (2011), 4307-4314

[35] R. Golovchak, A. Kovalskiy, A.C. Miller, H. Jain and O. Shpotyuk, *Phys. Rev. B*, *76*, (2007), 125208

[36] R. Golovchaka, O. Shpotyuka, J.S. Mccloy, B.J. Riley, C.F. Windisch, S.K. Sundaram, A. Kovalskiy and H. Jain, *Phil. Mag.*, 90 [34], 4489-4501

[37] G. Lucovsky, F. L. Galeener, R. C. Keezer, R. H. Geils, H. A. Six, *Phys. Rev. B*, *10*, (1974), 5134

[38] E. Bychkov, M. Miloshova, D.L. Price, C.J. Benmore and A. Lorriaux, *J. Non-Cryst. Solids*, *352*, (2006), 63-70

[39] T.G. Edwards, S. Sen, E.L. Gjersing, *J. Non-Cryst. Solids*, *358*, (2012), 609-614,

[40] J.C. Phillips, *J. Non-Cryst. Solids*, 34, (1979), 153-181

[41] H. He and M.F. Thorpe, *Phys. Rev. Lett.*, *54*, (1985), 2107-2110

[42] B.L. Halfpap and S.M. Lindsay, *Phys. Rev. Lett.*, 57, (1986), 847-9

[43] S. Gapochenko and V. Bazakutsa, *J. Non-Cryst. Solids*, *270*, (2000), 274 – 277

[44] P. Boolchand, R.N. Enzweiler, R.L. Cappelletti, W.A. Kamitakahara, Y. Cai and

M.F. Thorpe, Solid State Ionics, *39*, (1990), 81-89

[45] A.N. Sreeram, A.K. Varshneya and D.R. Swiler, *J. Non-Cryst. Solids*, *128*, (1991), 294 – 309

[46] P.K. Gupta and J.C. Mauro J. C., *J. Chem. Phys.*, *130*, (2009), 094503/1-094503/8

[47] Grüneisen 1st Rule," pp. 90. In *Physical Properties of Solid Materials*. Edited by C.Zwikker. Wiley Interscience, New York, 1954

[48] T. Rouxel, *C. R. Mecanique,* 334, (2006), 743-753

[49] E. V. Shkol'nikov, *Sov. J. Glass Phys. Chem.*, 11, (1985), 40-44

[50] G. Yang, B. Bureau, T. Rouxel, Y. Gueguen, O. Gulbiten, C. Roiland, E. Soignard, J.L. Yarger, J. Troles, J.-C. Sangleboeuf and P. Lucas, *Phys. Rev. B*, 82, (2010), 195206

[51] P. Boolchand and W.J. Bresser, *Phil. Mag. B*, 80 [10] , (2000), 1757-1772

Figure captions

Figure 1: *DSC curves and (b) Composition dependence of Tg for Ge_xSe_{1-x} glasses.*

Figure 2: *Composition dependence of (a) Young's modulus E, shear modulus G, and (b) Poisson's ratio v.*

Figure 3: *Density and atomic volume of Ge_xSe_{1-x} glasses.*

Figure 4: *(a) Compositional dependences of refractive index. (b) Compositional dependences of optical band gap in Ge_xSe_{1-x} glassy system.*

Figure 5: *Composition dependence of the mean atomic bonding energy obtained experimentally from K and V_0 (U_{0exp}) compared with theoretical values predicted from a continuously reticulated structure using bonding energies reported in ref. [49] (U_{01}) & [29] (U_{02}).*

Figure 6: *Composition dependence of the experimental and theoretical mean atomic bonding energy density for Ge_xSe_{1-x} glasses. The lines are fitting. The Ge crystal has a mean bonding energy ranging between 24 and 28 kJ/cm^3.*

Figure 7: *(a) Composition dependence of density of Ge_xSe_{1-x} glasses in the Ge-rich region and crystals, (b) Composition dependence of the mean atomic bonding energy density for crystals. The lines are guides to eye.*

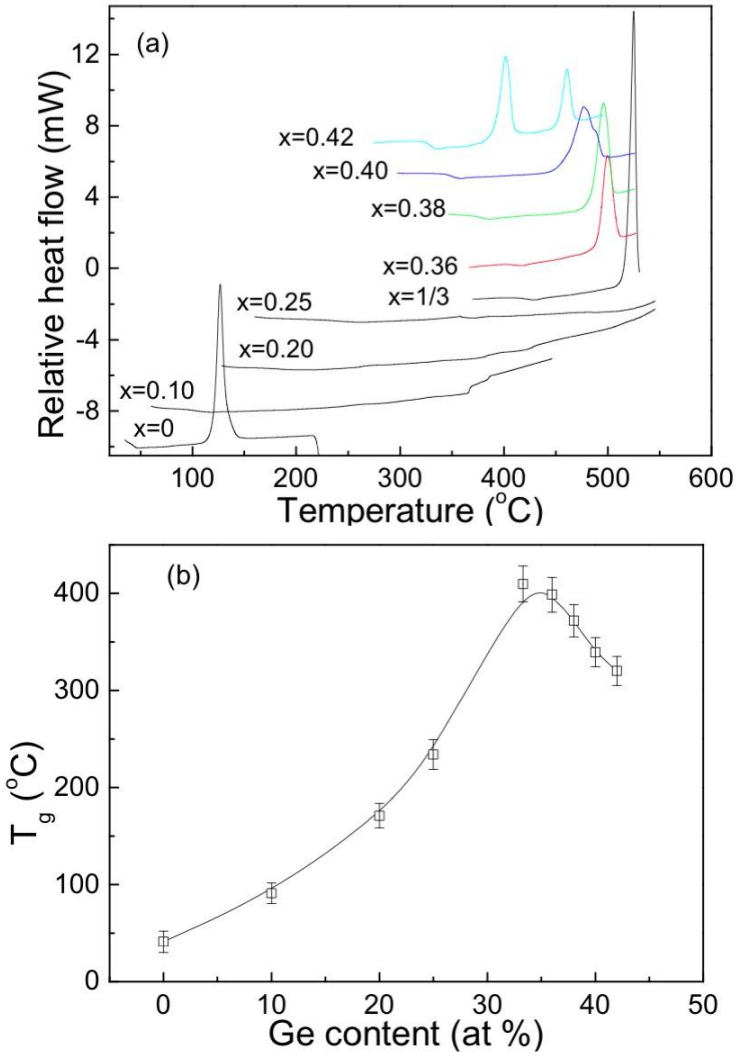

465 Figure 1

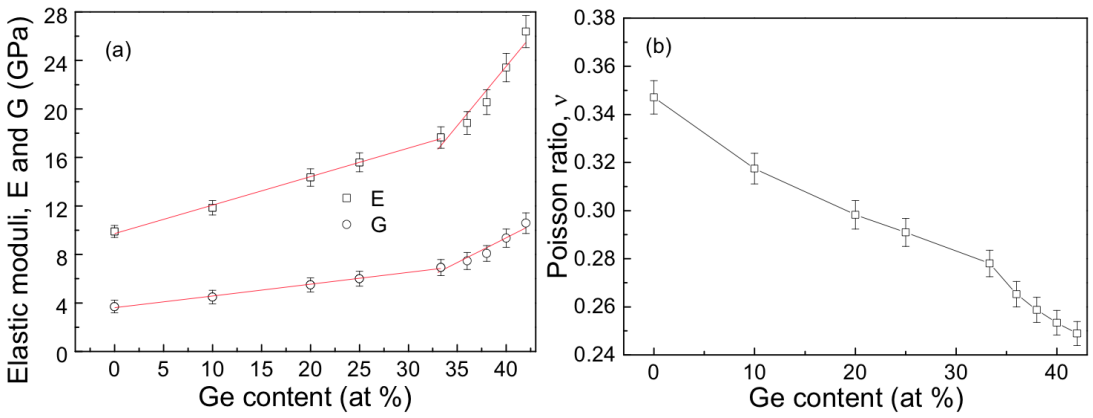

Figure 2

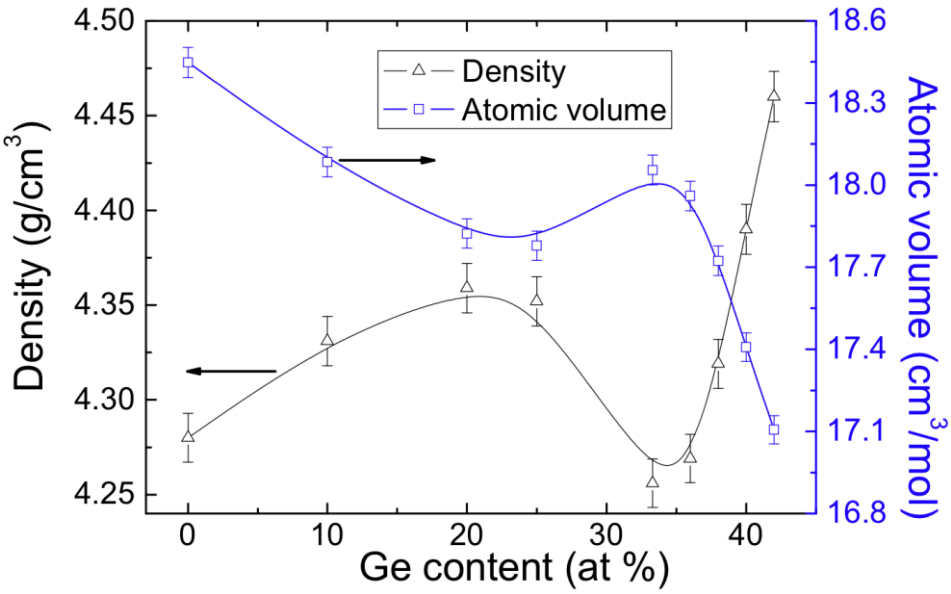

Figure 3

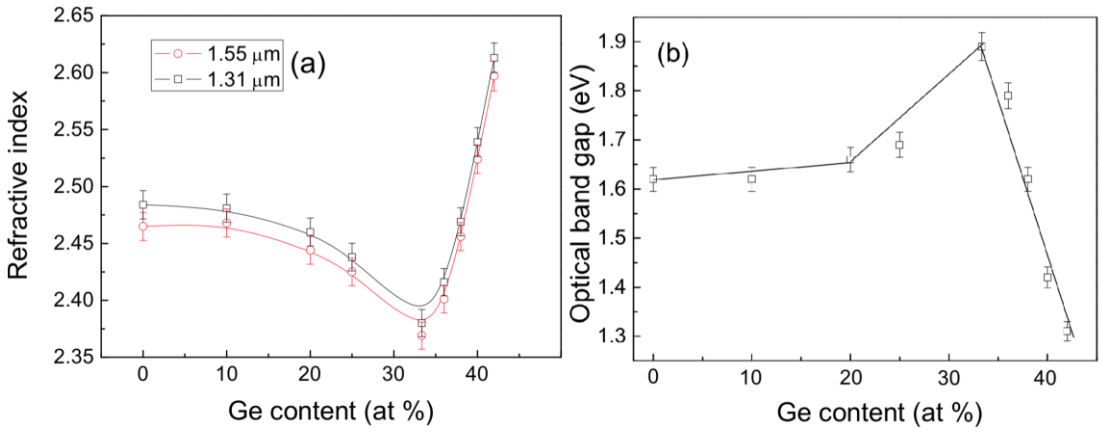

Figure 4

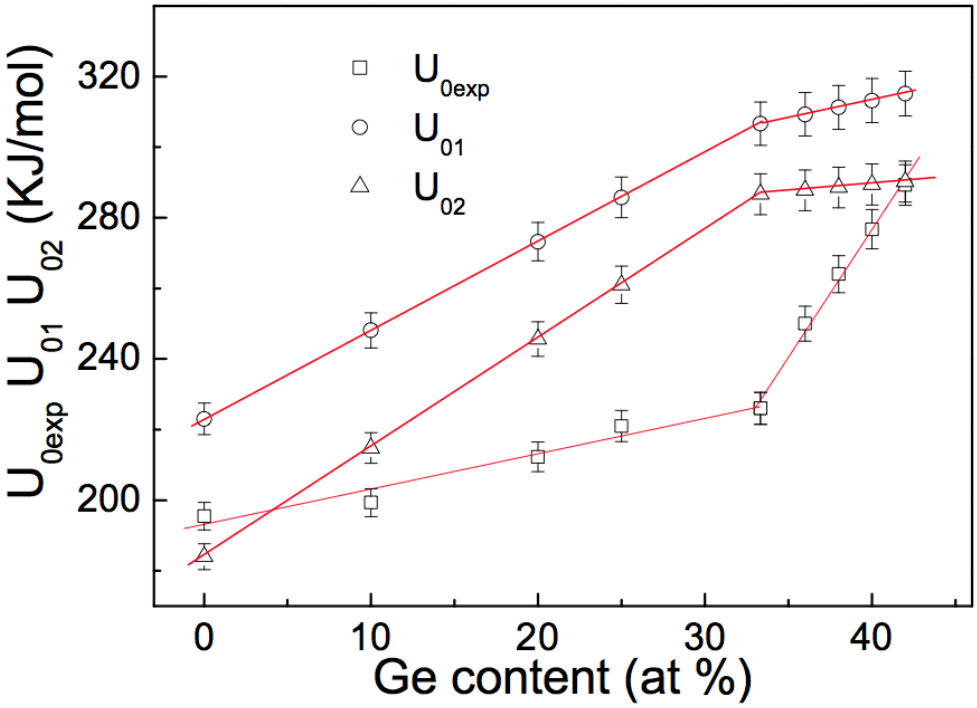

Figure 5

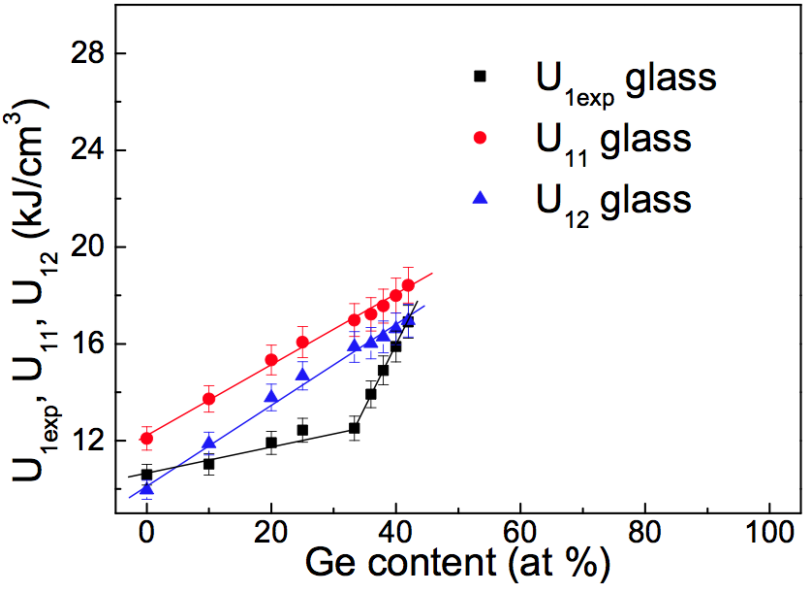

Figure 6

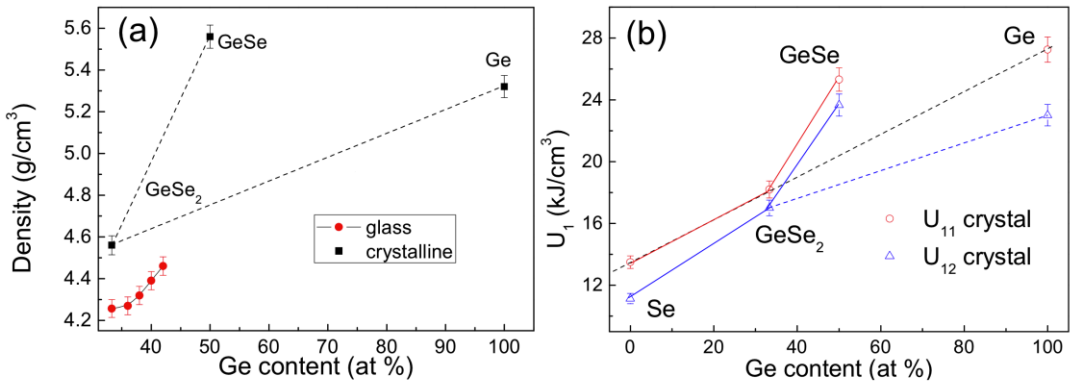
(a)
GeSe
Ge
GeSe2
glass
crystalline
Density (g/cm3)
Ge content (at %)
(b)
GeSe
Ge
GeSe2
Se
U11 crystal
U12 crystal
U1 (kJ/cm3)
Ge content (at %)

Figure 7